Synthesis of Novel Molybdaboranes from (η^5-C_5R_5)$MoCl_n$ Precursors (R = H, Me; n = 1, 2, 4)

Simon Aldridge,* Maoyu Shang, and Thomas P. Fehlner*

Contribution from the Department of Chemistry and Biochemistry, University of Notre Dame, Notre Dame, Indiana 46556

Received October 27, 1997

Abstract: Reaction of Cp*$MoCl_4$ (**1**), or (Cp*$MoCl_2$)$_2$ (**2**), Cp* = η^5-C_5Me_5, with BH_3·THF ultimately generates the Mo(II) cluster (Cp*Mo)$_2B_5H_9$ (**7**), together with the Mo(III) species (Cp*$MoCl$)$_2B_4H_{10}$, **4**. Prereduction of **2** before reaction with BH_3·THF yields only **7**. The structure of **4** consists of two Cp*Mo units bridged by two chlorides and a $[B_2H_5(B_2H_5)]^{2-}$ ligand in which the two diboron moieties are connected by a B−B−B three center bond. Closer inspection of the reaction by ^{11}B and ^{1}H NMR reveals the existence of three intermediate species (Cp*$MoCl$)$_2B_2H_6$ (**3**), (Cp*$MoCl$)$_2B_3H_7$ (**5**), and (Cp*Mo)$_2$(B_2H_6)$_2$ (**6**). Each of these species has been characterized spectroscopically, and crystal structures have been obtained for **3** and **5**. Compound **3** features molybdenum centers bridged by two chlorides and an ethane-like $[B_2H_6]^{2-}$ ligand such that the B−B bond is perpendicular to the Mo−Mo bond. Replacing one terminal H by $[B_2H_5]$ generates **4**. The structure of **5** is based on a trigonal bipyramidal Mo_2B_3 core, and the molecule is electronically unsaturated although the Mo−Mo distance (3.096 Å) precludes the existence of multiple bonding between the metal centers. **5** exists as a relatively stable molecule despite having too few electrons and too few atoms to adopt a capped structure based on a polyhedron with fewer vertexes. Comparison of MO descriptions of the electronic structure of **5** with that of the later transition metal species (Cp*Co)$_2B_3H_7$ (**8**) shows that this stabilization is derived from the appropriate energy match between Cp*Mo and borane based orbitals which elevates the energy of the Mo−B antibonding LUMO, a cluster orbital which would normally be filled, into the region of unoccupied orbitals. The concentration vs time behavior for the final products **4** and **7**, for the intermediates **3**, **5**, and **6**, for the monoboron species BH_3·THF and BH_2Cl, and selected non-boron containing species is used to define a pathway for the molybdaborane cluster condensation. With **1**, use of $LiBH_4$ as the monoboron source yields **6** as the primary product via **3** as an intermediate, whereas prereduction of **2** with $[Et_3BH]^-$ results in the formation of **7**. The varied cluster building abilities of BH_3·THF vs $LiBH_4$ originate in the differing reduction and coordination properties of the two monoboranes. Investigation of the analogous Cp = η^5-C_5H_5 system reveals similar chemistry albeit simpler and on a shorter time scale.

Introduction

Metallaboranes that incorporate metals to the left of iron are a relatively sparsely explored area of cluster chemistry.[1−4] Previous to this work, with the exception of coordination complexes containing the BH_4^-,[5] $B_3H_8^-$,[6] or $B_2H_4(PR_3)_2$[7] ligands, structurally authenticated compounds of the group 6 metals are confined to the electronically unsaturated chromaborane (Cp*Cr)$_2B_4H_8$ (Cp* = η^5-C_5Me_5)[8] and its derivatives[9−11] and to the molybdaboranes (Cp′Mo)$_2B_5H_9$ (Cp′ = η^5-C_5H_4Me),[12] $Cp_2Mo(H)B_2H_5$,[13] CpMo(η^5:η^1-C_5H_4)B_4H_7[14] and CpMo(η^3:η^2-C_3H_3)$C_2B_9H_9$ (Cp = η^5-C_5H_5).[14]

The challenge of the early transition metals is to find synthetic routes. That is, traditional synthetic routes to metallaboranes have focused on two broad but complementary approaches,[1−4] namely (i) insertion or fragmentation reactions of "ready-assembled" borane frameworks and (ii) condensation reactions of monoboron precursors. Typically, products are isolated by chromatography from reaction mixtures in low yields owing to the accessibility of several minima on the reaction pathway under the conditions employed.[15] Only the most stable/least reactive compounds are characterized greatly restricting the scope of the chemistry particularly when early transition metals are of interest.

Recently we have illustrated the use of dimeric metal-containing precursors as a method of controlling the number of

(1) Kennedy, J. D. *Prog. Inorg. Chem.* **1984**, *32*, 519.
(2) Kennedy, J. D. *Prog. Inorg. Chem.* **1986**, *34*, 211.
(3) Housecroft, C. E.; Fehlner, T. P. *Adv. Organomet. Chem.* 1**982**, *21*, 57.
(4) Grimes, R. N. In *Metal Interactions with Boron Clusters*; Grimes, R. N., Ed.; Plenum: New York, 1982; p 269.
(5) Marks, T. J.; Kolb, J. R. *Chem. Rev.* **1977**, *77*, 263.
(6) Guggenberger, L. J. *Inorg. Chem.* **1970**, *9*, 367.
(7) Shimoi, M.; Katoh, K.; Ogino, H. *J. Chem. Soc., Chem. Commun.* **1990**, 811.
(8) Deck, K. J.; Nishihara, Y.; Shang, M.; Fehlner, T. P. *J. Am. Chem. Soc.* **1995**, *117*, 10292.
(9) Hashimoto, H.; Shang, M.; Fehlner, T. P. *J. Am. Chem. Soc.* **1996**, *118*, 8164.
(10) Hashimoto, H.; Shang, M.; Fehlner, T. P. *Organometallics* **1996**, *15*, 1963.
(11) Aldridge, S.; Hashimoto, H.; Kawamura, K.; Shang, M.; Fehlner, T. P. *Inorg. Chem.* In press.
(12) Bullick, H. J.; Grebenik, P. D.; Green, M. L. H.; Hughes, A. K.; Leach, J. B.; McGowan, P. C. *J. Chem. Soc., Dalton Trans.* **1995**, 67.
(13) Grebenik, P. D.; Green, M. L. H.; Kelland, M. A.; Leach, J. B.; Mountford, P.; Stringer, G.; Walker, N. M.; Wong, L. L. *J. Chem. Soc., Chem. Commun.* **1988**, 799.
(14) Grebenik, P. D.; Leach, J. B.; Kelland, M. A.; Green, M. L. H.; Mountford, P. *J. Chem. Soc., Chem. Commun.* **1989**, 1397.
(15) Meng, X.; Bandyopadhyay, A. K.; Fehlner, T. P.; Grevels, F.-W. *J. Organomet. Chem.* **1990**, *394*, 15.

S0002-7863(97)03720-7 CCC: $15.00
Published on Web 03/05/1998

Table 1. ^{11}B NMR of the Metallaboranes **3**−**7**[a,b]

	3[c]	**4**[c]		**5**[c]	**6**	**7**
B−M	*d*	*d*		105.5 {155} B(1)	*d*	62.9 {130} (3B, accid. overlap of two signals)
B−H−M	−44.1 [290, 200] B(1), B(2)	−56.7 [760, 630]	B(2)	34.2	−58.6	25.8 (2B)
		−27.2 [910, 550]	B(1)	B(2), B(2′)	[220, 190] (all 4B)	
		−11.9 [1320, 720] −8.0 [1440, 1020]	B(3), B(4)			

[a] Toluene solutions at 21 °C for **3**−**6**; hexane solution at 21 °C for **7**. [b] Coupling constant $J(^{11}B-^{1}H)$ in Hz given where appropriate in the form {150}; fwhm in Hz given in the form [290, 200] refers to the coupled and ^{1}H decoupled spectra, respectively. [c] Numbering scheme for each molecule taken from the appropriate figure. [d] Not applicable.

Table 2. ^{1}H NMR of the Metallaboranes **3**−**7**[a,b]

	3	**4**	**5**	**6**	**7**
B−*H*−M	−13.4 (4)	−12.6 (2), −12.1 (2)	−4.8 (4, 70)	−12.4 (8)	−7.0 (4)
B−*H*	1.1 (2, 120)	0.4 (1) ≈2.5 (4), ≈3.6 (1)	3.4 (2), 8.5 (1)	0.6 (4, 130)	3.9 (1), 5.37 (2), 6.22 (2)

[a] Relative intensities and coupling constants $J(^{11}B-^{1}H)$ in Hz where appropriate given in parentheses. [b] Solutions in [$^{2}H_6$]benzene at 21 °C.

metal atoms in the product during condensation reactions of BH_3·THF.[8,16] The extension of this approach to molybdenum species of the type $(Cp^*MoCl_n)_2$ offers a promising route to clusters of the stoichiometry Mo_2B_x. Using this method we have been successful in isolating Mo_2B_2, Mo_2B_3,[17] Mo_2B_4,[18] and Mo_2B_5[18] metallaboranes. These high yield reactions permit mechanistic studies of cluster condensation from halogenated precursors including the role of Cp* vs Cp ligand on the reaction chemistry. To this end qualitative experiments have been carried out resulting in the identification of at least three intermediate species (all of which have been subsequently isolated and two crystallographically characterized). This allows the delineation of the pathway of the stepwise build-up of metallaborane clusters thereby defining the similarities and differences of borane and borohydride as cluster building units.

A key intermediate in the formation of one final product $(Cp^*Mo)_2B_5H_9$ is the electronically unsaturated species $(Cp^*MoCl)_2B_3H_7$.[17] This cluster is of interest not only because of its role as a reaction intermediate but also as a rare example of a metallaborane which has insufficient skeletal electrons based on the Wade-Mingos rules to justify its observed molecular structure.[19,20] It is the first such unsaturated metallaborane for which a later transition metal analogue exists containing the same borane fragment [$(Cp^*Co)_2B_3H_7$[16]]; this allows identification of the electronic factors stabilizing the unsaturated cluster.

Experimental Section

General Methods. All manipulations were carried out under a nitrogen or argon atmosphere using standard Schlenk line or drybox techniques. Solvents were predried over 4-Å molecular sieves (tetrahydrofuran) or KOH (hexanes, toluene) and purged with nitrogen prior to distillation. Tetrahydrofuran (THF), toluene, and hexanes were all distilled from sodium benzophenone ketal. Starting materials for the molybdaboranes, Cp^*MoCl_4 (**1**) or $(Cp^*MoCl_2)_2$ (**2**), were prepared according to the methods of King,[21] Schrock,[22] and Green.[23] The analogous Cp compounds $CpMoCl_4$ (**1′**) and $(CpMoCl_2)_n$ (**2′**) were also prepared according to literature methods.[22,24−26] The BH_3·THF and $LiBH_4$ solutions (Aldrich) were used as received without further purification.

NMR spectra were measured on a Varian-300 or Varian-500 FT-NMR spectrometer. Residual protons of solvent were used for reference for ^{1}H NMR (δ, ppm: benzene, 7.15; toluene, 2.09), while a sealed tube containing $[(NEt_4)(B_3H_8)]$ (δ_B −29.7 ppm) was used as the external reference for ^{11}B NMR. Infrared spectra were measured on a Nicolet 205 FT-IR spectrometer. Mass spectra were measured on a JEOL JMS-AX 505HA mass spectrometer using the EI ionization mode. Perfluorokerosene was used as the standard for high-resolution EI mass spectra.

Synthesis of Final Molybdaborane Products. ^{11}B and ^{1}H NMR data for the molybdaboranes **3**−**7** are listed in Tables 1 and 2, respectively.

(i) $(Cp^*MoCl)_2B_4H_{10}$ (4). Reaction of $(Cp^*MoCl_2)_2$ (**2**) with a 5-fold excess of BH_3·THF in toluene at 45 °C for 120 h yields a mixture of **4** and **7**, as determined by ^{11}B NMR spectroscopy.[18] **7** is easily removed by washing with hexane, and crystals of **4** can then be grown by layering a toluene solution with hexane (yield ca. 45% based on the amount of **2** taken). An identical mixture of products **4** and **7** is obtained on treating Cp^*MoCl_4 (**1**) with 7 equiv of BH_3·THF under similar reaction conditions. **4** has been characterized by ^{11}B and ^{1}H NMR, solid-state IR, mass spectrometry, and single-crystal X-ray diffraction.[18] Additional spectroscopic data for **4**: MS (EI), $P^+ = 587$, two Mo, two Cl, four B atoms, calcd for weighted average of 81 isotopomers falling within the resolution limits of the spectrometer at the measured ion peak, 587.1078, obsd 587.1107. IR (KBr, cm^{-1}) 2979 m, 2960 m, 2912 s, 2857 w sh, ν(C−H); 2493 s, 2462 s, 2624 vs, ν(B−H_t); 1994 m br, ν(B−H_b); 1376 s, 1028 m, δ(CH_3).

(ii) $(Cp^*Mo)_2B_5H_9$ (7). Although the synthesis of $(C_5H_4MeMo)_2B_5H_9$ in 0.75−1.5% yield has previously been reported by the reaction of $C_5H_4MeMoCl_4$ with $LiBH_4$ in diethyl ether,[12] $(Cp^*Mo)_2B_5H_9$ (**7**) is most conveniently prepared by the reaction of either Cp^*MoCl_4 (**1**), $(Cp^*MoCl_2)_2$ (**2**), or "[Cp*MoCl]" with BH_3·THF.[18] Reaction of **1** with a 7-fold excess of BH_3·THF in toluene at 45 °C over a period of 120 h yields a mixture of **7** and the Mo(III) metallaborane $(Cp^*MoCl)_2B_4H_{10}$ (**4**),[18] from which **7** is easily separated by extraction with hexane. Concentration of a hexane solution followed by cooling to −40 °C allows orange crystals of **7** to be isolated in yields of 30−40% based on the amount of **1** taken. Reaction of $(Cp^*MoCl_2)_2$ (**2**) with BH_3·THF under similar conditions gives an identical mixture of the products **4** and **7**. On the other hand, reduction of **2** (140 mg, 0.23 mmol) by 2 equiv of $LiEt_3BH$ in toluene at room temperature [to yield the Mo(II) halide "Cp*MoCl"] followed by removal of volatiles in vacuo and subsequent reaction with a 3-fold excess of BH_3·THF (also in toluene) produced an orange solution from which tiny orange crystals of $(Cp^*Mo)_2B_5H_9$ could be isolated as the only metallaborane product

(16) Nishihara, Y.; Deck, K. D.; Shang, M.; Fehlner, T. P.; Haggerty, B. S.; Rheingold, A. L. *Organometallics*, **1994**, *13*, 4510.
(17) Aldridge, S.; Shang, M.; Fehlner, T. P. *J. Am. Chem. Soc.* **1997**, *119*, 11120.
(18) Aldridge, S.; Fehlner, T. P.; Shang, M. *J. Am. Chem. Soc.* **1997**, *119*, 2339.
(19) Wade, K. *New Scientist* **1974**, *62*, 615.
(20) Mingos, D. M. P. *Acc. Chem. Res.* **1984**, *17*, 311.
(21) King, R. B.; Bisnette, M. B. *J. Organomet. Chem* **1967**, *8*, 287.
(22) Murray, R. C.; Blum, L.; Liu, A. H.; Schrock, R. R. *Organometallics* **1985**, *4*, 953.
(23) Green, M. L. H.; Hubert, J. D.; Mountford, P. *J. Chem. Soc., Dalton Trans.* **1990**, 3793.
(24) Cousins, M.; Green, M. L. H. *J. Chem. Soc.* 1964, 1567.
(25) Krueger, S. T.; Owens, B. E.; Poli, R. *Inorg. Chem*. **1990**, *29*, 2001.
(26) Linck, R. G.; Owens, B. E.; Poli, R.; Rheingold, A. L. *Gazz. Chim. Ital.* **1991**, *121*, 163.

Table 3. Amounts of Reagents Used for ^{11}B NMR-Monitored Reactions

	amount of reagents used				
	Cp*$MoCl_4$	BH_3·THF[a]	toluene (cm^3)	overall concn of BH_3·THF (M)	ratio Cp*$MoCl_4$:BH_3·THF
1	20 mg, 0.054 mmol	1.08 cm^3, 0.216 mmol	1.08	0.1	1:4
2	20 mg, 0.054 mmol	1.35 cm^3, 0.270 mmol	1.35	0.1	1:5
3	20 mg, 0.054 mmol	1.89 cm^3, 0.378 mmol	1.89	0.1	1:7

[a] 0.2 M solution in THF.

[i.e., none of the Mo(III) cluster **4** was formed]. By contrast, the reaction of **1** with 5 equiv of $LiBH_4$, analogous to that reported by Green et al. in their synthesis of $(C_5H_4MeMo)_2B_5H_9$ gives very low yields of the Mo_2B_5 cluster **7**, the predominant product being the bis-(B_2H_6) adduct **6** (vide infra). Characterization of **7** was achieved by comparison of the measured NMR spectra with those reported for $(C_5H_4MeMo)_2B_5H_9$.[12]

Synthesis and Isolation of Intermediate Species. NMR experiments revealed the existence of three intermediates in the formation of $(Cp^*Mo)_2B_5H_9$ (**7**) and $(Cp^*MoCl)_2B_4H_{10}$ (**4**) by the reaction of Cp*$MoCl_4$ (**1**) with 7 equiv of BH_3·THF. These were subsequently shown to be $(Cp^*MoCl)_2B_2H_6$ (**3**), $(Cp^*MoCl)_2B_3H_7$ (**5**), and $(Cp^*Mo)_2(B_2H_6)_2$ (**6**). If only 4 equiv of BH_3·THF are used, then the concentrations of these intermediates do not fall to zero, and the concentrations of the final products **4** and **7** remain low even after long reaction times (ca. 6 days). It seems probable that there is insufficient BH_3·THF present under these conditions to convert all of the intermediate species formed to the final products **4** and **7**.

(i) $(Cp^*MoCl)_2B_2H_6$ (3). By optimizing the reaction conditions (45 °C, 6 days reaction time, 4:1 ratio of BH_3·THF:**1**) it proved possible to obtain a reaction mixture in which by far the largest component (as determined by ^{11}B NMR) was the intermediate **3**. Removal of volatiles in vacuo at this point and extraction into hexane gave a green-brown solution and an insoluble brown solid (which was subsequently shown by ^{1}H NMR to be unreacted **2**). Repeated concentration and cooling of the hexane solution gave dark brown crystals of **3** in yields of 15−18% based on the amount of **1** taken. **3** has been characterized by ^{11}B and ^{1}H NMR, mass spectrometry, and single-crystal X-ray diffraction. An added complication was the presence of ≈14% of **2** which cocrystallizes with **3**, the existence of which is shown by ^{1}H NMR spectra and which complicates the interpretation of the crystal structure data. The initial single crystals examined contained ≈85% of **2**, and repeated recrystallization was required to reduce the impurity level to acceptable limits. Additional spectroscopic data for **3**: MS(EI), P^+ = 560, two Mo, two B, two Cl atoms; isotopic distribution in excellent agreement with formulation $C_{20}H_{36}B_2Cl_2Mo_2$.

(ii) $(Cp^*MoCl)_2B_3H_7$ (5). Of the three intermediate species **5** is present in the lowest concentration at all reaction times, presumably because its electronic unsaturation renders it extremely reactive to further BH_3·THF (vide infra). Only by the use of more dilute reaction mixtures (containing lower concentrations of BH_3·THF) did it prove possible to isolate this intermediate and then only in low yield. Accordingly, reaction of Cp*$MoCl_4$ (**1**) with 4 equiv of BH_3·THF in a dilute toluene solution (ca. 50 mM in BH_3·THF) at 55 °C over a period of 72 h produces the cluster **5** in ca. 5% yield. Removal of volatiles in vacuo, extraction with hexane, and filtration yields a solution containing a mixture of **3**−**5** from which the dark green microcrystalline product **5** can be isolated by cooling to −10 °C (**5** is less soluble in hexane than either **3** or **4**). Dissolution in toluene and layering of the solution with hexane allows the growth of rectangular platelike crystals of **5** by slow diffusion over a period of 2−3 days at room temperature. **5** has been characterized by ^{11}B and ^{1}H NMR, IR spectroscopy, and single-crystal X-ray diffraction. Additional spectroscopic data for **5**: IR (KBr, cm^{-1}) 2982 w, 2962 w, 2916 s, 2855 w sh, ν(C−H); 2498 s, 2455 s, ν(B−H_t); 1475 m, 1448 w sh, 1415 w, 1377 s, 1071 w, δ-(CH_3); 752 s, 675 w sh, 664 m, ρ(CH_3) [δ = deformation mode, ρ = rocking mode]. Attempts to obtain the mass spectrum of **5** were frustrated by its extreme air and moisture sensitivity.

(iii) $(Cp^*Mo)_2(B_2H_6)_2$ (6). Although the molybdaborane **6** has been identified as an intermediate in the formation of **7** by the reaction of Cp*$MoCl_4$ (**1**) with 7 equiv of BH_3·THF, the most convenient synthesis of **6** is by the reaction of **1** with 10 equiv of $LiBH_4$ in toluene. The solution of $LiBH_4$ in thf was added to a solution/suspension of **1** in toluene at −80 °C, and the reaction mixture was allowed to warm slowly to room temperature. After 72 h **6** was shown to be the predominant metallaborane product by ^{11}B NMR (there being less than 5% of the Mo_2B_5 species **7**), and volatiles were removed in vacuo to yield a brown solid. Extraction with hexane, concentration of the resulting brown solution, and cooling to −10 °C gave a brown microcrystalline precipitate of **6**. All attempts to obtain a crystalline sample of **6** suitable for study by X-ray diffraction instead gave microcrystalline material. **6** has been characterized by ^{11}B and ^{1}H NMR and mass spectrometry. Additional spectroscopic data for **6**: MS(EI), P^+ = 518, two Mo, four B, atoms; isotopic distribution in excellent agreement with formulation $C_{20}H_{42}B_2Mo_2$.

NMR-Monitored Reactions. To investigate possible mechanistic pathways linking the fully halogenated starting material Cp*$MoCl_4$ (**1**) and the metallaborane end-products $(Cp^*MoCl)_2B_4H_{10}$ (**4**) and $(Cp^*Mo)_2B_5H_9$ (**7**) a series of experiments was carried out in which the reaction mixture was monitored periodically by NMR. Reaction mixtures were made up in 10 mm NMR tubes as listed in Table 3—the total amount of **1** in each was kept constant as was the *concentration* of BH_3·THF, but the ratio of **1**:BH_3·THF was varied by using a different volume of borane solution in each tube. The BH_3·THF solution was added to the solution/suspension of **1** in toluene at −40 °C, and the reaction mixture was allowed to warm to room temperature. After 90 min at room temperature the reaction temperature was raised to 55 °C for the remainder of the experiment, and the composition of the reaction mixture monitored periodically by ^{11}B NMR.

A further experiment was carried out in which the reaction was monitored by ^{1}H NMR in order to reveal the concentration/time dependence for ^{11}B silent species such as $(Cp^*MoCl_2)_2$ and possible molybdenum hydride intermediates. To this end 10 mg (0.03 mmol) of **1** was loaded into a 5 mm NMR tube and 1.0 cm^3 of [^{2}H$_6$]benzene was added; to this solution/suspension was added BH_3·THF (0.11 mmol). Both the ratio of **1**:BH_3·THF (1:4) and the concentrations of the reagents used were the same as those used in tube 1 of the ^{11}B NMR-monitored reaction, although in order to allow for the smaller volume of the 5 mm tube the absolute quantities of all reagents were reduced from those used for the 10 mm tube reaction. As before, the first 90 min of reaction time were at room temperature with the tube subsequently being heated to 55 °C for the remainder of the experiment; the composition of the reaction mixture was monitored periodically by ^{1}H NMR.

Cp Analogues. Reactions of the corresponding cyclopentadienyl molybdenum species $CpMoCl_4$ (**1′**) and $(CpMoCl_2)_n$ (**2′**) with a large excess of BH_3·THF (7 or 5 equiv, respectively) were also investigated by ^{11}B NMR spectroscopy. In each case only one intermediate and one final product was observed. The final product is characterized by three ^{11}B NMR signals (2:1:2) at δ_B 61.0, 59.4 [both doublets, J(^{11}B−^{1}H) ≈ 140 Hz], and 27.1 (broad multiplet); the observed spectrum is assigned to **7′** as it is essentially identical to that reported for $(C_5H_4MeMo)_2B_5H_9$[12] and $(Cp^*Mo)_2B_5H_9$ (**7**). The only intermediate detected gives rise to a single ^{11}B NMR signal at δ_B −45.4 (**3′**) [broad doublet, J(^{11}B−^{1}H) ≈ 140 Hz]; the reaction is considerably faster than in the Cp* case—at room temperature the concentration of the intermediate species is maximized after a 24 h reaction time and is completely consumed after 72 h.

Use of $LiBH_4$ as the Boron Source. The reaction of $C_5H_4MeMoCl_4$ with 3.5 equiv of $LiBH_4$ in diethyl ether has been previously investigated by Green et al. who isolated $(C_5H_4MeMo)_2B_5H_9$ in 0.75−1.5% yield.[12] We have repeated the reaction using toluene as the solvent

Table 4. Crystal Data and Structure Refinement Details for Compounds **3**−**5**

	3	**4**	**5**
formula weight	560.92	586.54	572.71
crystal system	monoclinic	monoclinic	tetragonal
space group	$P2_1$	$P2_1/c$	$P4_32_12$
a (Å)	8.1278(7)	11.5162(11)	8.5231(13)
b (Å)	29.447(6)	15.261(2)	8.5231(13)
c (Å)	10.601(4)	14.815(2)	32.956(7)
β (deg)	108.61(3)	103.183(10)	
V (Å^3)	2404.6(10)	2535.1(5)	2394.0(7)
Z	4	4	4
ρ_{calcd} (g cm^{-3})	1.565	1.537	1.589
$F(000)$	1146	1192	1160
wavelength (Å)	0.71073	0.71073	0.71073
abs. coeff (mm^{-1})	1.298	1.205	1.275
crystal size (mm)	0.48 × 0.18 × 0.02	0.25 × 0.16 × 0.10	0.40 × 0.33 × 0.02
θ range (deg)	2.03−28.39	2.25−22.99	2.47−24.96
index ranges	$-9 \le h \le 10$	$0 \le h \le 12$	$0 \le h \le 10$
	$-30 \le k \le 37$	$0 \le k \le 16$	$0 \le k \le 10$
	$-13 \le l \le 10$	$-16 \le l \le 15$	$0 \le l \le 39$
no. of reflns collected	9999	3717	2422
no. of independent reflns	6360	3523	2099
	[R(int) = 0.0606]	[R(int) = 0.0587]	[R(int) = 0.0497]
no. of observed reflns[a]	4952	2910	1826
refinement method	full-matrix on F^2	full-matrix on F^2	full-matrix on F^2
data/restraints/parameters	6342/95/526	3522/19/284	2099/0/137
goodness of fit on F^2	1.094	1.216	1.143
final R indices [$I > 2\sigma(I)$]	$R_1 = 0.0683$	$R_1 = 0.0708$	$R_1 = 0.0420$
	w$R_2 = 0.1466$	w$R_2 = 0.2148$	w$R_2 = 0.0944$
R indices (all data)[b]	$R_1 = 0.0982$	$R_1 = 0.0830$	$R_1 = 0.0542$
	w$R_2 = 0.1745$	w$R_2 = 0.2290$	w$R_2 = 0.1053$
largest diff. peak and hole (e Å^{-3})	0.985 and −0.935	1.270 and −1.848	0.934 and −0.472

[a] [$I > 2\sigma(I)$]. [b] wR2 = $\{[\sum w(F_c^2 - F_o^2)^2]/[\sum w(F_o^2)^2]\}^{1/2}$.

and monitoring the progress of the reaction by ^{11}B NMR. Using 3.5 equiv of $LiBH_4$, added to a solution/suspension of Cp^*MoCl_4 at −78 °C and warming to room temperature, the ^{11}B NMR spectrum measured after 30 min indicates the presence of both **3** and **6**, together with a small amount of unreacted $LiBH_4$ and a much larger quantity of BH_3·-THF, presumably produced during the initial reduction of Cp^*MoCl_4 to $(Cp^*MoCl_2)_2$ by $LiBH_4$ (vide infra). At longer reaction times the concentration of **3** falls (such that after 72 h there is very little of this species remaining), whereas the concentration of **6** continues to grow. After 72 h the ^{11}B spectrum reveals that **6** is the predominant metallaborane species in solution, there being additional weak signals due to the Mo_2B_5 species **7**. Conversion of **6** to **7** is very slow even at 55 °C, such that **6** remains the major component of the mixture even after several weeks and the addition of further aliquots of $LiBH_4$. If the reaction is carried out with 10 equiv of $LiBH_4$ (rather than 3.5), then the maximum concentration achieved by the intermediate **3** is much lower, and the amount of **7** ultimately produced is also lower.

X-ray Structure Determinations. Details of the data collection and structure refinement procedures for compounds **3**−**5** are summarized in Table 4. Data collection for compounds **4** and **5** was carried out using an Enraf-Nonius CAD4 diffractometer, whereas that for **3** was carried out on an Enraf-Nonius FAST area detector diffractometer; all data were collected at room temperature.

$(Cp^*MoCl)_2B_4H_{10}$ (4). A dark green-brown acicular crystal of **7** was grown by slow diffusion of hexane into a concentrated toluene solution at −40 °C over a period of 6 days and mounted on a glass fiber prior to data collection. Most of the non-hydrogen atoms were located by direct methods and the remainder found in successive difference Fourier syntheses. All non-hydrogen atoms were refined anisotropically and all hydrogen atoms were then located in a difference Fourier map. Both borane and methyl hydrogens were included in the final refinement, the former being treated isotropically with bond length restraints, the latter as idealized riding atoms [r(C−H) = 0.96 Å, U_{iso}(H) = 1.5 U_{eq}(C)]. The structure was refined on F^2 by full-matrix least-squares methods using SHELXTL V5.[27] Selected bond distances are listed in Table 5; other data have been deposited in conjunction with the original communication.[18]

$(Cp^*MoCl)_2B_2H_6$ (3). A brown platelike crystal of **3** was grown by cooling a concentrated hexane solution to −10 °C over a period of 4 days and mounted on a glass fiber for data collection. Most of the non-hydrogen atoms were shown on an E-map; ensuing least-squares refinement and successive difference Fourier syntheses revealed the remaining non-hydrogen atoms and the disorder model of a B_2H_6 group with two bridging chlorine atoms in each of the independent Mo_2 cluster

Table 5. Selected Interatomic Distances (Å) and Angles (deg) for $(Cp^*MoCl)_2B_4H_{10}$ (**4**)

	Distance		
Mo(1)−C(1)	2.228(12)	Mo(2)−C(15)	2.328(11)
Mo(1)−C(2)	2.273(11)	Mo(2)−B(1)	2.44(2)
Mo(1)−C(3)	2.324(12)	Mo(2)−B(2)	2.422(13)
Mo(1)−C(4)	2.342(12)	Mo(2)−Cl(1)	2.463(3)
Mo(1)−C(5)	2.254(13)	Mo(2)−Cl(2)	2.478(3)
Mo(1)−B(1)	2.42(2)	Mo(2)−H(3)	1.80(2)
Mo(1)−B(2)	2.42(2)	Mo(2)−H(5)	1.80(2)
Mo(1)−Cl(1)	2.468(3)	B(1)−B(2)	1.70(2)
Mo(1)−Cl(2)	2.486(3)	B(1)−H(1)	1.06(2)
Mo(1)−Mo(2)	2.7113(13)	B(1)−H(2)	1.08(2)
Mo(1)−H(2)	1.82(2)	B(1)−H(3)	1.05(2)
Mo(1)−H(4)	1.80(2)	B(2)−B(3)	1.77(2)
Mo(2)−C(11)	2.270(12)	B(2)−B(4)	1.87(2)
Mo(2)−C(12)	2.228(11)	B(2)−H(4)	1.05(2)
Mo(2)−C(13)	2.262(10)	B(2)−H(5)	1.05(2)
Mo(2)−C(14)	2.348(11)	B(3)−B(4)	1.79(3)
	Angle		
C(1)−Mo(1)−B(1)	97.9(5)	C(12)−Mo(2)−B(1)	153.7(5)
C(2)−Mo(1)−B(1)	125.7(5)	C(13)−Mo(2)−B(1)	116.3(5)
C(3)−Mo(1)−B(1)	158.4(5)	C(14)−Mo(2)−B(1)	97.0(5)
C(4)−Mo(1)−B(1)	136.3(6)	C(15)−Mo(2)−B(1)	110.3(5)
C(5)−Mo(1)−B(1)	102.8(5)	C(11)−Mo(2)−B(2)	117.1(5)
C(1)−Mo(1)−B(2)	98.0(5)	C(13)−Mo(2)−B(2)	142.7(5)
C(2)−Mo(1)−B(2)	103.2(4)	C(14)−Mo(2)−B(2)	108.1(5)
C(3)−Mo(1)−B(2)	135.7(5)	C(15)−Mo(2)−B(2)	96.5(5)
C(4)−Mo(1)−B(2)	158.9(5)	Cl(1)−Mo(2)−Cl(2)	76.46(12)
C(5)−Mo(1)−B(2)	126.1(5)	Mo(2)−Cl(1)−Mo(1)	66.71(8)
Cl(1)−Mo(1)−Cl(2)	76.21(12)	Mo(2)−Cl(2)−Mo(1)	66.21(8)
B(1)−Mo(1)−Mo(2)	56.4(4)	B(1)−B(2)−B(3)	82.9(11)
B(2)−Mo(1)−Mo(2)	56.0(3)	B(1)−B(2)−B(4)	141.3(12)
B(1)−Mo(1)−B(2)	41.2(5)	B(3)−B(2)−B(4)	58.6(10)
B(1)−Mo(2)−B(2)	41.1(5)	B(3)−B(4)−B(2)	58.0(9)
C(11)−Mo(2)−B(1)	145.1(5)		

(27) SHELXTL.-V5; Siemens Industrial Automation Inc.: 1994.

Table 6. Selected Interatomic Distances (Å) and Angles (deg) for $(Cp^*MoCl)_2B_2H_6$ (**3**)

		Distance	
Mo(1)−C(1)	2.27(2)	Mo(2)−B(2)	2.40(2)
Mo(1)−C(2)	2.24(2)	Mo(2)−Cl(2)	2.493(5)
Mo(1)−C(3)	2.18(2)	Mo(2)−Cl(1)	2.502(5)
Mo(1)−C(4)	2.29(2)	Mo(2)−H(13)	1.8(2)
Mo(1)−C(5)	2.36(2)	Mo(2)−H(23)	1.6(2)
Mo(1)−B(1)	2.34(2)	B(1)−B(2)	1.63(3)
Mo(1)−B(2)	2.42(3)	B(1)−H(11)	1.37(5)
Mo(1)−Cl(2)	2.474(5)	B(1)−H(12)	1.36(5)
Mo(1)−Cl(1)	2.490(5)	B(1)−H(13)	1.36(5)
Mo(1)−Mo(2)	2.696(2)	B(2)−H(21)	1.36(5)
Mo(1)−H(12)	1.6(2)	B(2)−H(22)	1.37(5)
Mo(1)−H(22)	1.8(2)	B(2)−H(23)	1.37(5)
Mo(2)−B(1)	2.37(2)		
		Angle	
C(1)−Mo(1)−B(1)	103.1(9)	B(2)−Mo(1)−Cl(1)	85.6(7)
C(2)−Mo(1)−B(1)	98.9(9)	B(2)−Mo(1)−Cl(2)	109.6(6)
C(3)−Mo(1)−B(1)	126.6(9)	Cl(2)−Mo(1)−Cl(1)	76.3(2)
C(4)−Mo(1)−B(1)	156.8(8)	B(1)−Mo(1)−Mo(2)	55.7(6)
C(5)−Mo(1)−B(1)	135.8(9)	B(2)−Mo(1)−Mo(2)	55.6(6)
C(1)−Mo(1)−B(2)	125.2(9)	B(2)−B(1)−Mo(1)	72.7(14)
C(2)−Mo(1)−B(2)	98.8(9)	B(2)−B(1)−Mo(2)	71.0(12)
C(3)−Mo(1)−B(2)	103.8(8)	Mo(1)−B(1)−Mo(2)	69.8(6)
C(4)−Mo(1)−B(2)	136.2(8)	B(1)−B(2)−Mo(2)	69.2(11)
C(5)−Mo(1)−B(2)	156.5(8)	B(1)−B(2)−Mo(1)	67.4(13)
B(1)−Mo(1)−B(2)	39.9(8)	Mo(2)−B(2)−Mo(1)	68.0(7)
B(1)−Mo(1)−Cl(1)	110.0(7)	Mo(1)−Cl(1)−Mo(2)	65.37(13)
B(1)−Mo(1)−Cl(2)	84.8(6)	Mo(1)−Cl(2)−Mo(2)	65.74(12)

units. Note: The ratio of cocrystallized **3** and **2** is ≈6 as independently determined from ^{1}H NMR of the single crystals used. In the refinement free variables were used to restrain divergence of the B−B and Cl···Cl distances. After all non-hydrogen atoms were refined anisotropically, all hydrogen atoms were then located in a difference Fourier map. Both borane and methyl hydrogens were included in the final refinement, the former being treated isotropically with bond length restraints, the latter as idealized riding atoms [r(C−H) = 0.96 Å, U_{iso}(H) = 1.5 U_{eq}(C)]. The structure was refined on F^2 by full-matrix least-squares methods using SHELXTL V5.[27] Coordinates and selected bond distances are listed in Tables S2 (Supporting Information) and 6, respectively.

$(Cp^*MoCl)_2B_3H_7$ (5). A dark green platelike crystal of **5** was grown by slow diffusion of hexane into a concentrated toluene solution at room temperature over a period of 2−3 days and mounted in a capillary under argon prior to data collection. Most of the non-hydrogen atoms were located by direct methods, and the remainder found in successive difference Fourier syntheses. All non-hydrogen atoms were refined anisotropically, and all hydrogen atoms were then located in a difference Fourier map. Both borane and methyl hydrogens were included in the final refinement, the former being treated isotropically, the latter as idealized riding atoms [r(C−H) = 0.96 Å, U_{iso}(H) = 1.5 U_{eq}(C)]. The structure was refined on F^2 by full-matrix least-squares methods using SHELXTL V5.[27] Selected bond distances are listed in Table 7; other data have been deposited in conjunction with the original communication.[17]

MO Calculations. Fenske−Hall calculations[28,29] were carried out for the molecules $(CpMoCl)_2B_3H_7$ (**3′**) and $(CpCo)_2B_3H_7$ (**8′**); in both cases the geometry used was that derived from the solid-state structure determination of the corresponding Cp* (η^5-C_5Me_5) derivative (including hydrogen atom positions) with the simplification that the permethylated Cp* ligand was replaced by Cp (η^5-C_5H_5).[15,24] For both molecules **3′** and **8′** the minimal atomic orbital (AO) basis set calculations were transformed into fragment basis sets for two CpM (M = MoCl or Co) and B_3H_7 fragments.

Results and Discussion

Synthesis and Characterization of New Molybdaboranes. The results of the reactions of the pentamethylcyclopentadienyl molybdenum halides **1** and **2** with monoboron reagents are summarized in Schemes 1−3. The structures shown are based upon analyses of the spectroscopic and crystallographic data which follow. The reaction pathway is based upon the results of NMR-monitored experiments which are described subsequently.

Table 7. Selected Interatomic Distances (Å) and Angles (deg) for $(Cp^*MoCl)_2B_3H_7$ (**3**)[a]

		Distance	
Mo−B(1)	2.144(8)	Mo−H(3)	1.74(6)
Mo−B(2)#1	2.257(8)	B(1)−B(2)#1	1.838(11)
Mo−B(2)	2.286(8)	B(1)−B(2)	1.838(11)
Mo−C(1)	2.302(7)	B(1)−Mo#1	2.144(8)
Mo−C(5)	2.312(7)	B(1)−H(1)	1.06(14)
Mo−C(2)	2.353(8)	B(2)−Mo#1	2.257(8)
Mo−C(3)	2.355(6)	B(2)−H(2)	1.27(5)
Mo−C(4)	2.358(7)	B(2)−H(3)	1.26(6)
Mo−Cl	2.423(2)	B(2)−H(4)	1.06(7)
Mo−Mo#1	3.0958(12)		
		Angle	
B(1)−Mo−B(2)#1	49.3(3)	B(2)#1−Mo−C(5)	149.1(3)
B(1)−Mo−B(2)	48.9(3)	B(1)−Mo−Cl	135.3(2)
B(2)#1−Mo−B(2)	87.7(3)	B(2)−Mo−Cl	98.3(3)
B(1)−Mo−C(1)	89.6(3)	B(2)#1−Mo−Cl	112.1(3)
B(1)−Mo−C(2)	82.1(3)	B(1)−Mo−Mo#1	43.8(2)
B(1)−Mo−C(3)	109.8(3)	B(2)#1−Mo−Mo#1	47.4(2)
B(1)−Mo−C(4)	140.3(3)	B(2)−Mo−Mo#1	46.6(2)
B(1)−Mo−C(5)	124.5(3)	B(2)−B(1)−B(2)#1	117.8(9)
B(2)−Mo−C(1)	92.9(3)	B(2)#1−B(1)−Mo#1	69.6(4)
B(2)−Mo−C(2)	112.4(3)	B(2)−B(1)−Mo#1	68.5(4)
B(2)−Mo−C(3)	147.1(4)	B(2)#1−B(1)−Mo	68.5(4)
B(2)−Mo−C(4)	144.3(3)	B(2)−B(1)−Mo	69.6(4)
B(2)−Mo−C(5)	109.0(3)	Mo#1−B(1)−Mo	92.4(4)
B(2)#1−Mo−C(1)	120.7(3)	B(1)−B(2)−Mo#1	62.2(3)
B(2)#1−Mo−C(2)	90.9(3)	B(1)−B(2)−Mo	61.5(3)
B(2)#1−Mo−C(3)	93.2(3)	Mo#1−B(2)−Mo	85.9(3)
B(2)#1−Mo−C(4)	124.5(3)		

[a] Symmetry transformations used to generate equivalent atoms: #1 $y, x, -z+2$.

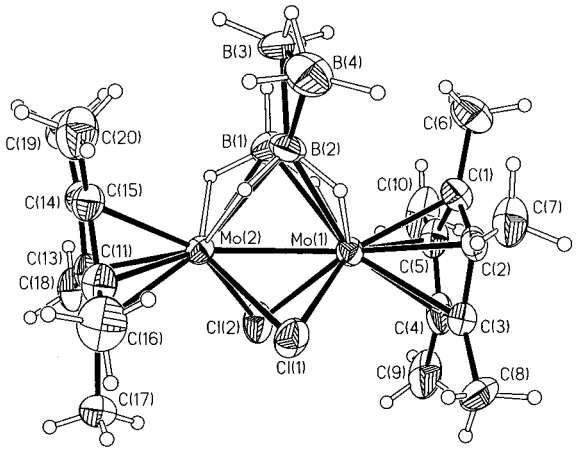

Figure 1. ORTEP drawing of $(Cp^*MoCl)_2B_4H_{10}$ (**4**).

$(Cp^*MoCl)_2B_4H_{10}$ (4). Reaction of **1** (or **2**) with a 7-fold (5-fold) excess of BH_3·THF generates two products which are easily separated by solubility.[18] The less hexane-soluble material has a molecular formula $(Cp^*MoCl)_2B_4H_{10}$, but the ^{11}B and ^{1}H NMR spectra imply a low symmetry structure featuring a single plane of symmetry. For this reason the structure was only defined by a single-crystal X-ray diffraction study, and it is given in Figure 1; relevant interatomic distances and angles are listed in Table 5. The structure is consistent with the observed spectroscopic data and shows two Cp*Mo units linked by a pair of bridging chloride ligands and in a side-on fashion

(28) Fenske, R. F. *Pure Appl. Chem.* **1988**, *27*, 61.
(29) Hall, M. B.; Fenske, R. F. *Inorg. Chem.* **1972**, *11*, 768.

by a B_4H_{10} unit. Bridging of the dimetal unit by B(1) and B(2) is reminiscent of the interaction of the $B_2H_6^{2-}$ ligand with a dinuclear group 5 unit in $(C_5Me_4EtNb)_2(B_2H_6)_2$,[30] (*p*-tolNCHN*p*-tol)$_4$Ta$_2$(B_2H_6),[31] $(Cp^*Ta)_2(B_2H_6)_2$,[32] and one form of $(Cp^*TaBr)_2B_2H_6$.[32] Comparison of the bonding parameters for **4** with analogous M_2B_2 units reveals B−B [1.70(2) Å] and B−H_b distances [1.05(2)−1.08(2) Å] which are within the range of values expected for this mode of coordination.[30,31] The similar M−B distances for the molybdenum [2.42(2)−2.44(2) Å], tantalum [2.48(1)−2.51(1) Å for (*p*-tolNCHN*p*-tol)$_4$Ta$_2$-(B_2H_6)[31]], and niobium [2.401(4)−2.408(4) Å for $(C_5Me_4EtNb)_2$-$(B_2H_6)_2$[30]] compounds reflect similar radii for the metals involved.[33]

The structure of **4** is viewed as a dimolybdenum unit bridged by two chlorides and by a $[B_2H_6]^{2-}$ ligand in which one single terminal hydrogen has been replaced by a μ-B_2H_5 fragment. In common with most other structurally characterized B_2H_5 units, the $H_2B\cdots BH_2$ unit is planar and approximately perpendicular to the plane defined by the $\overline{BBHB}$ unit. The B···B distance within the B_2H_5 unit [1.79(3) Å] is consistent with those obtained for other related compounds.[34−36] Furthermore, the B(2)−B(3) and B(2)−B(4) distances [1.77(2) and 1.87(2) Å, respectively] are similar to the analogous values in [CpCo(Me_3-Si)$_2C_2B_4H_3$][B_2H_5] [1.789(2) and 1.799(2) Å[35]] and also to those in B_3H_7CO [1.820(6) and 1.803(6) Å[36]]. In common with these compounds the B_2H_5 unit in **4** is viewed as being linked to the third boron atom via a three-center boron−boron−boron bond.

As a terminal hydrogen from an ethane-like $[B_2H_6]^{2-}$ unit has been replaced by B_2H_5, the bridging ligand is formally $B_4H_{10}^{2-}$, and the molybdenum centers are formally in the +III oxidation state. The ditantalum compound $(Cp^*TaBr)_2B_2H_6$[32] is said to have a Ta═Ta double bond suggesting a single bond between the two molybdenum centers in **4**. Similarities in the Mo−Mo bond length [2.711(1) Å] and Mo(μ-Cl)Mo angles [66.71(8), 66.21(8)°] of the Mo(μ-Cl)$_2$Mo unit with those reported for [($C_5H_4{}^iPr$)Mo(μ-Cl)$_2$]$_2$ [2.607(1) Å and 63.17(3), 63.34(3)°, respectively[37]] are consistent with a single bond linking two Mo(III) centers.

$(Cp^*Mo)_2B_5H_9$ (7). Of the two final products produced by the reaction of **1** (or **2**) with BH_3·THF, **7** is much more soluble in hexane. The NMR data are virtually identical to those reported for the structurally characterized molybdaborane (C_5H_4-MeMo)$_2B_5H_9$,[12] and the pattern of resonances is also very similar to that found for the chromaborane $(Cp^*Cr)_2B_5H_9$.[18] Both $(C_5H_4MeMo)_2B_5H_9$ and $(Cp^*Cr)_2B_5H_9$ are best viewed as 46 cve (six sep) clusters based around a $M_2B_3H_3$ trigonal bipyramidal core (M = Cr or Mo) capped by two BH_3 fragments,[11,12] and an analogous structure for **7** is therefore proposed on the basis of this spectroscopic evidence.

$(Cp^*MoCl)_2B_2H_6$ (3). Mass spectral data for **3** are consistent with the formulation $(Cp^*MoCl)_2B_2H_6$; the ^{11}B NMR spectrum indicates the presence of a single boron environment, and the chemical shift is consistent with hydrogen-bridged rather than direct Mo−B linkages. The ^{1}H NMR spectrum reveals a single Cp* resonance (relative intensity 30), a single Mo−H−B signal (intensity 4), and one BH resonance (intensity 2). The spectral data are consistent with an ethane-like $B_2H_6^{2-}$ unit symmetrically bridging a dimolybdenum framework as shown in Scheme 2. Similar spectra reported for the minor isomer of $(Cp^*TaBr)_2B_2H_6$[32] and for $(C_5Me_4EtNbCl)_2B_2H_6$,[30] together with the absence of any resonance attributable to a BHB hydrogen corroborate this assignment. In addition, the ^{11}B NMR shift and the ^{1}H NMR shift for the Mo−H−B protons are similar to those found in **4** which contains a related ethane-like B_2H_5R unit.

Scheme 1

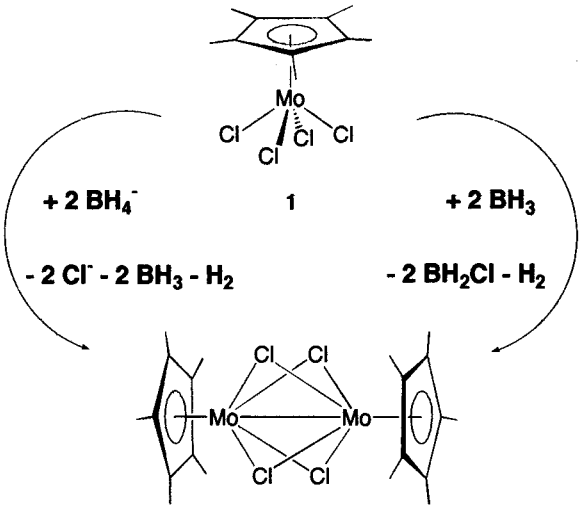

The single-crystal X-ray diffraction structure of **3** is reproduced in Figure 2; relevant interatomic distances and angles are listed in Table 6. The asymmetric unit contains two independent $(Cp^*MoCl)_2B_2H_6$ molecules which differ little in terms of geometric parameters (Table 6 lists parameters for only one of the two molecules). The structure is consistent with the observed spectroscopic data and shows two Cp*Mo units linked by a pair of bridging chloride ligands and in a side-on fashion by a B_2H_6 unit. The B−B distance [1.63(3) Å] is in the range expected for the directly bonded ethane-like $(H_3B-BH_3)^{2-}$ ligand predicted spectroscopically, being very slightly shorter than the corresponding distance in (*p*-tolNCHN*p*-tol)$_4$Ta$_2$(B_2H_6) [1.68(2) Å[31]] and markedly shorter than that observed for the hydrogen-bridged $(H_2BHBH_3)^{2-}$ ligand found for $(Cp^*TaBr)_2$-B_2H_6 in the solid state [1.88(3) Å[32]].

Viewed as a metallaborane cluster, **3** has the correct electron count for an M_2B_2 tetrahedron (six sep's or 40 cve); such a formulation implies a Mo−Mo bond, and the observed interatomic distance [2.696(2) Å] is consistent with this. **3** can therefore be seen as a tetrahedral Mo_2B_2 cluster with a doubly chloride-bridged Mo−Mo bond and four hydrogen-bridged Mo−B linkages. Alternatively, viewing **3** as a complex featuring two Mo(III) centers and a bridging $B_2H_6^{2-}$ ligand (isoelectronic with C_2H_6), the molybdenum centers each attain an 18-electron configuration by the formation of an Mo−Mo single bond. This requires the $B_2H_6^{2-}$ ligand to act as an eight-electron ligand (four to each metal center) which it accomplishes by utilizing four BH bonds each as a two-electron donor. This view of **3** is given further weight by the description of the analogous group 5 compounds $(Cp^*TaBr)_2B_2H_6$[32] and (C_5Me_4-$EtNbCl)_2B_2H_6$[30] as M═M doubly bonded dimers.

(30) Brunner, H.; Gehart, G.; Wachter, J.; Wrackmeyer, B.; Nuber, B.; Ziegler, M. L. *J. Organomet. Chem.* **1992**, *436*, 313.
(31) Cotton, F. A.; Daniels, L. M.; Murillo, C. A.; Wang, X. *J. Am. Chem. Soc.* **1996**, *118*, 4830.
(32) Ting, C.; Messerle, L. *J. Am. Chem. Soc.* **1989**, *111*, 3449.
(33) Huheey, J. E. *Inorganic Chemistry; Principles of Structure and Reactivity*; Harper and Row: New York, 1972.
(34) Borelli, A. J.; Plotkin, J. S.; Sneddon, L. G. *Inorg. Chem.* **1982**, *21*, 1328−1331.
(35) Briguglio, J. J.; Sneddon, L. G. *Organometallics* **1985** *4*, 721.
(36) Glore, J. D.; Rathke, J. W.; Schaeffer, R. *Inorg. Chem.* **1973**, *12*, 2175.
(37) Grebenik, P. D.; Green, M. L. H.; Izquierdo, A.; Mtetwa, V. S. B.; Prout, K. *J. Chem. Soc., Chem. Commun.* **1987**, 9.

Scheme 2

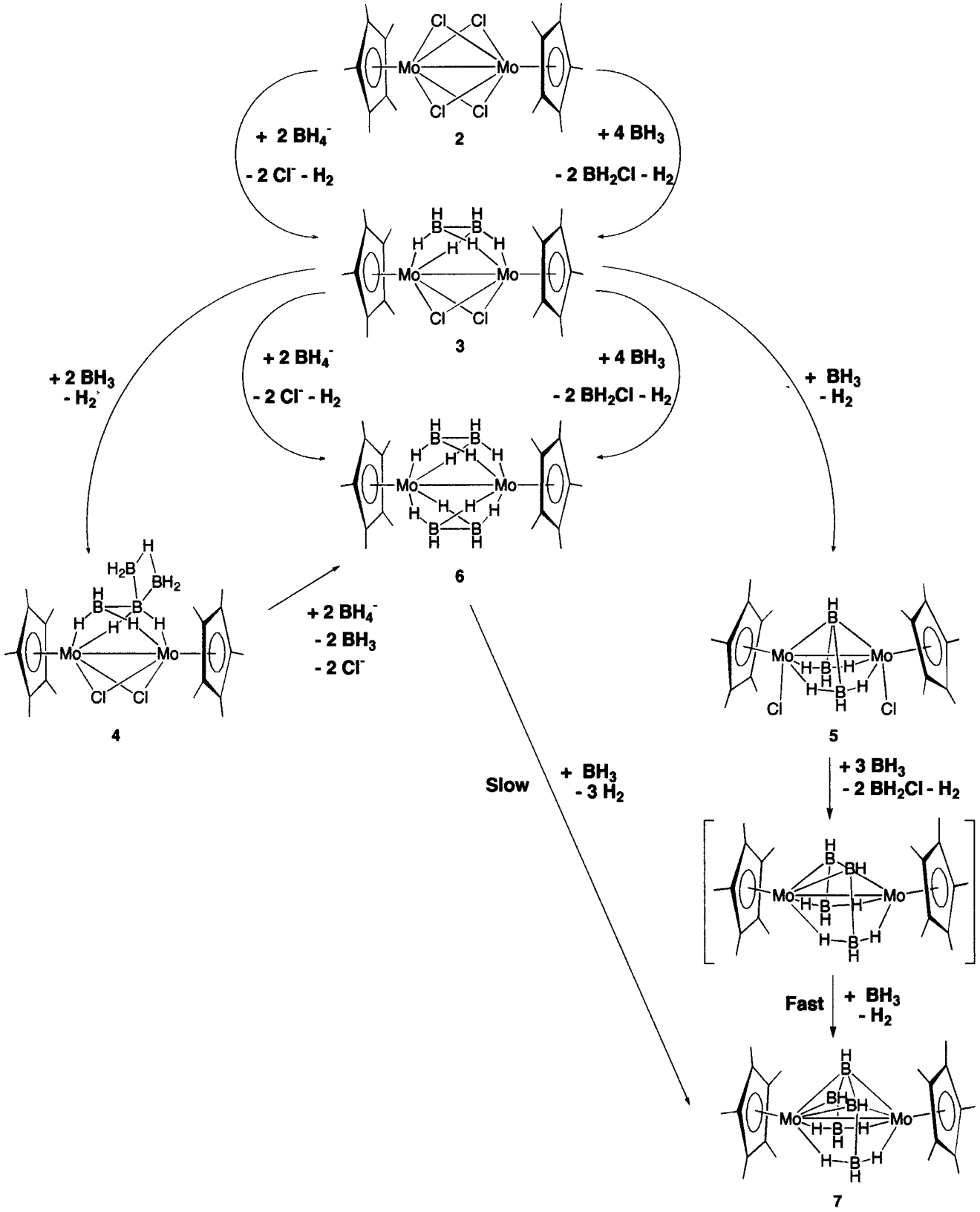

$(Cp^*MoCl)_2B_3H_7$ (5). Of the three intermediate species identified, **5** is present in the lowest concentration and is by far the most sensitive to air and moisture.[17] Mass spectral data and ^{11}B and ^{1}H NMR data are consistent with the molecular structure shown in Scheme 2. This is confirmed by a single-crystal X-ray diffraction structure reproduced in Figure 3; relevant interatomic distances and angles are listed in Table 7. The structure of **5** is best viewed as a trigonal bipyramid; the required number of skeletal electron pairs is six (42 cve), and since the electron count for $(Cp^*MoCl)_2B_3H_7$ is only five pairs (40 cve) this implies that the molecule is electronically unsaturated.

Comparison of the structural metrics of **5** with those of the saturated species $\{(C_5H_4Me)Mo\}_2B_5H_9$[12] reveals a longer Mo−

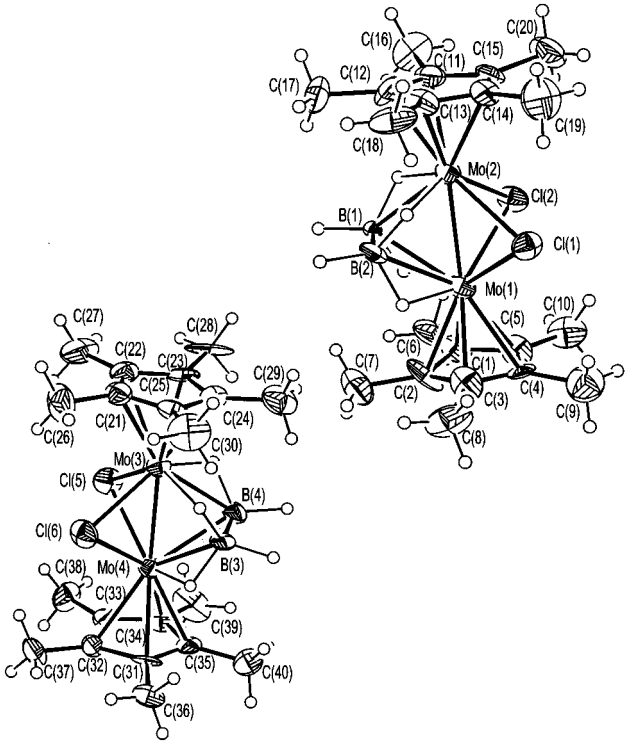

Figure 2. ORTEP drawing of the two independent molecules making up the asymmetric unit of $(Cp^*MoCl)_2B_2H_6$ (**3**).

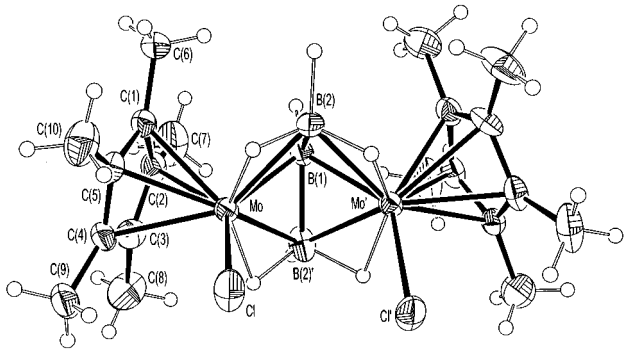

Figure 3. ORTEP drawing of $(Cp^*MoCl)_2B_3H_7$ (**5**).

Mo distance [3.0958(12) vs 2.812(1) Å] and shorter M−B distances. The former precludes multiple bonding between the molybdenum centers which is one possible response to electronic unsaturation. That is, species containing triple or quadruple bonds between molybdenum centers typically have internuclear distances of less than 2.5 Å [e.g., $(Me_3SiCH_2)_3Mo{\equiv}Mo(CH_2SiMe_3)$, 2.167 Å;[38] $Me(Me_2N)_2Mo{\equiv}Mo(NMe_2)_2Me$, 2.201 Å;[39] $Me_2(Me_3P)_2Mo{\equiv}Mo(PMe_3)_2Me_2$, 2.153 Å[40]]. On the other hand, the observed Mo−Mo distance of **5** is shorter than that observed in both $[CpMo(CO)_3]_2$ (3.22 Å[41]) and $Mo_2(CO)_{10}^{2-}$ (3.123 Å[42]) with metal−metal single bonds and much shorter than the 3.575 Å found in the cation $[\{(MeO)_3P\}_2(OC)_2Mo(\mu\text{-}Cl)_3Mo(CO)_2\{P(OMe)_3\}_2]^{n+}$ which has no Mo−Mo bond.[43] The B−B distances are considerably longer for the **5** than for $\{(C_5H_4Me)Mo\}_2B_5H_9$. The principal geometric differences between saturated $\{(C_5H_4Me)Mo\}_2B_5H_9$ and unsaturated **5** are mirrored by similar changes between saturated and unsaturated derivatives of the Cr_2B_4 system.[8,44]

Comparison with the seven skeletal pair dicobalt species $(Cp^*Co)_2B_3H_7$ (**8**)[16] is instructive. The differences between the two species are consistent with the differing electron counts. Corresponding to its predicted *nido* structure, the Co−Co distance in $(Cp^*Co)_2B_3H_7$ is long and nonbonding, and the B−B−B angle is 100.6(7)° which approximates that expected for three boron atoms on adjacent vertexes of an octahedron. In **5** the Mo−Mo distance is shorter and, as indicated above, Mo−Mo bonding. In addition, the B_3 ligand is more "opened out" in **5** than in $(Cp^*Co)_2B_3H_7$ with longer B−B distances and a wider B−B−B angle [117.8(9)°]. Both differences are consistent with the two Mo atoms and three boron atoms of **5** occupying two equatorial and two apical and one equatorial positions, respectively, of a trigonal bipyramid.

Interestingly, the two chloride ligands in **5** adopt terminal positions, rather than the μ_2-bridging coordination mode seen for both chlorides in **3** and **4**. In the latter compounds the four extra electrons supplied by the chlorides adopting μ_2-bridging rather than terminal positions allows the skeletal electron count to reach the six pairs required for a tetrahedron-based structure. In **5** the presence of an extra BH group in the cluster (B_3H_7 vs B_2H_6, in effect) means that the electron pair count would be five with two terminal chlorides or seven if both were μ_2-bridging. The steric requirement of the B_3H_7 ligand is clearly greater than that of B_2H_6 and this may force the chlorides to adopt terminal positions with the consequence that the Mo−Mo distance is longer [3.096(1) Å for **5** vs. 2.696(2) for 3 and 2.710(1), 2.690(2) Å for **4**] and the angle between the two Cp* rings is larger [49.7(2)° for **5** vs 1.5(8), 4.9(9) for **3** and 9.85° for **4**].

$(Cp^*Mo)_2(B_2H_6)_2$ (6). In addition to being one of three intermediates in the formation of **4** and **7** from Cp^*MoCl_4, **1**, $(Cp^*Mo)_2(B_2H_6)_2$ (**6**) is the predominant product of the reaction of **1** with $LiBH_4$, being formed in ca. 70% yield when 10 equiv of the borohydride are used. **6** is converted slowly to the Mo_2B_5 species **7** by reaction with further $LiBH_4$ at 55 °C over a period of several weeks. Mass spectral data for **6** are consistent with the formulation $(Cp^*Mo)_2(B_2H_6)_2$, and the single signal observed in the ^{11}B NMR spectrum indicates a highly symmetrical structure in solution. Three ^1H NMR signals are observed with the intensity ratio 15:4:2 attributed to the Cp*, MoHB, and BH protons, respectively. These spectral data are consistent with a dimeric $(Cp^*Mo)_2$ unit symmetrically bridged by a pair of equivalent ethane-like B_2H_6 units as shown in Scheme 2.

Electronic Structure of an Unsaturated Molybdaborane. Fenske−Hall molecular orbital (MO) calculations were carried out in order to determine (i) why the unsaturated species **5** is stable despite having two fewer electrons than required by the Wade-Mingos rules; (ii) why the metallaborane clusters **5** and **8** are both stable despite skeletal electron counts differing by two pairs; and (iii) why the two examples of unsaturated metallaboranes synthesized to date (**5** and $(Cp^*Cr)_2B_4H_8$, **9**) display similar geometric changes with respect to saturated analogues (i.e., lengthening of the M−M bond and shortening of M−B linkages).

Relevant sections of the eigenvalue spectra calculated for $(CpMoCl)_2B_3H_7$ (**5′**) and $(CpCo)_2B_3H_7$ (**8′**) by Fenske−Hall molecular orbital methods are reproduced in Figure 4. Also

(38) Huq, F.; Mowat, W.; Shortland, A.; Skapski, A. C.; Wilkinson, G. *J. Chem. Soc., Chem. Commun.* **1971**, 1079.
(39) Girolami, G. S.; Mainz, V. V.; Andersen, R. A.; Vollmer, S. H.; Day, V. W. *J. Am. Chem. Soc*. **1981**, *103*, 3953.
(40) Chisholm, M. H.; Cotton, F. A.; Extine, M. W.; Murillo, C. A. *Inorg. Chem.* **1978**, *17*, 2338.
(41) Gould, R. O.; Barker, J.; Kilner, M. *Acta Crystallogr.* **1988**, *C44*, 461.
(42) Handy, L. B.; Ruff, J. K.; Dahl, L. F. *J. Am. Chem. Soc.* **1970**, *92*, 7312.
(43) Drew, M. G. B. *J. Chem. Soc., Dalton Trans*. **1975**, 1984.
(44) Fehlner, T. P. *J. Organomet. Chem.* In press.

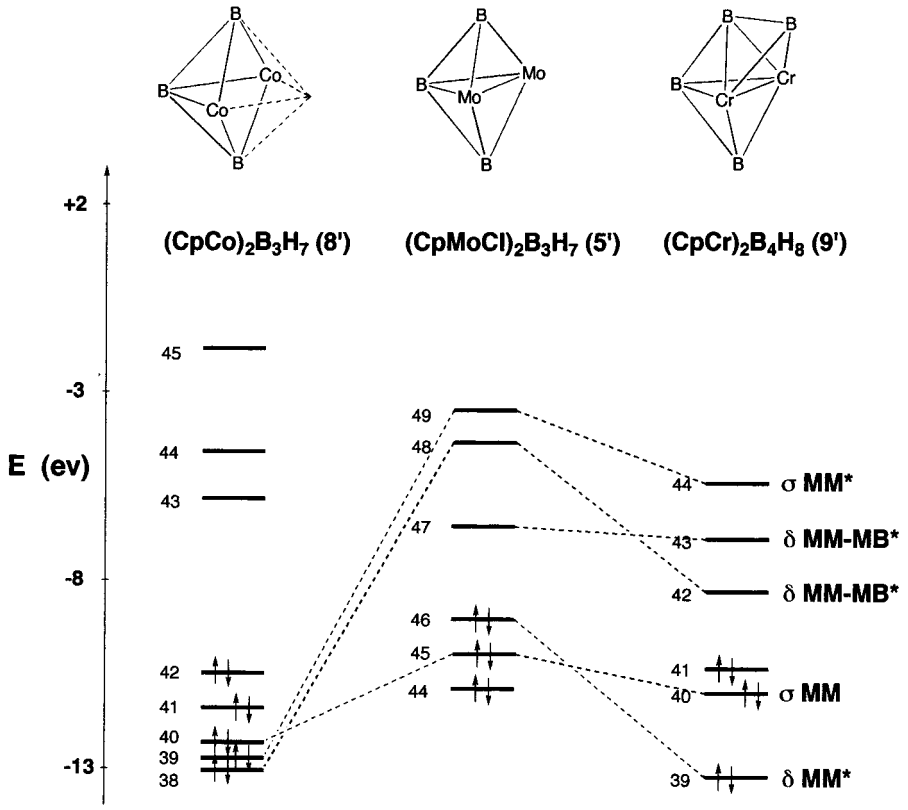

Figure 4. Molecular orbital scheme for $(CpMoCl)_2B_3H_7$ (**5′**), $(CpCo)_2B_3H_7$ (**8′**), and $(CpCr)_2B_4H_8$ (**9′**).

included is part of the MO scheme calculated previously for the unsaturated chromaborane $(CpCr)_2B_4H_8$ (**9′**).[8,44] Consistent with the stability of both **8′** and **5′**, a comparison of the MO pictures reveals a significant HOMO/LUMO gap for the saturated **8′** as expected as well as for the unsaturated **5′**.

In **5′** MOs 45 and 49 constitute a Mo−Mo σ bonding/antibonding pair of orbitals; MO 45 is low-lying and filled, whereas MO 49 is high-lying and empty. The corresponding pair of orbitals in **8′** constitute part of the filled, nonbonding set lying at low energy. In essence, the Mo−Mo bonding interaction implied by the MO diagram is consistent with the Mo−Mo distance as well as the view of **5** as based on a trigonal bipyramidal geometry, i.e., one of the two extra pairs of electrons present in the *nido* cobalt system is unneeded in the *closo* molybdenum system. The other pair of pertinent orbitals is occupied MO 38 for **8′**, which lies at −12.94 eV, and unoccupied MO for **5′** (48) at −4.27 eV. Both MOs are M−B antibonding and the occupation numbers agree with the differences in M−B distances observed in the structures. The large difference in energy between the two MOs is traced to the difference in energies of the 3d functions of the two metals and the differences in cluster geometry. In the case of Co the 3d functions are more core-like and low-lying. For Cr they are found at higher energy and are a better match in energy and size for the borane fragment orbitals thereby enhancing the M−B antibonding character of MO 48. The net result is that **5′** has two fewer bonding MOs and two fewer skeletal pairs than **8′**.

Similar orbital interactions account for the unsaturation in $(CpCr)_2B_4H_8$ (**9′**). Relative to the saturated chromaboranes $(CpCr)_2B_4H_8Fe(CO)_3$ and $(CpCr)_2B_4H_6(CO)_2$, there is a lengthening of the Cr−Cr bond and shortening of the Cr−B bonds.[9,44] Since the LUMO for **9′** is Cr−Cr bonding and Cr−B antibonding, it is found at high energy and unoccupied. As the corresponding orbital is occupied in its saturated counterparts, **9′** has one fewer occupied MO.[44] Further, the MO description of the metal−metal bonding in **5′** and **9′** is similar. The pleasing correspondence between the geometric and MO characteristics of **5** and **9** corroborates the description of these compounds as unsaturated metallaboranes.

Pathways for Reaction of $[Cp^*MoCl_n]$, $n = 1, 2, 4$, with Monoboranes. The reaction of the monocyclopentadienyl molybdenum halides **1**, **2**, and [CpMoCl] (produced by the stoichiometric reduction of **2** with $[Et_3BH]^-$)[18] with BH_3·THF have been examined by multinuclear NMR. Further the reaction of $LiBH_4$ with **1** and [CpMoCl] have been examined in like manner. The results are summarized in Schemes 1−3 (BH_3·THF is represented by BH_3 and $LiBH_4$ by BH_4^-) and discussed below. The compounds in brackets are postulated intermediates—all other compounds have been isolated and characterized as described above.

Borane. The reduction of **2** with 2 mol of $[Et_3BH]^-$ followed by the removal of the Et_3B and treatment with BH_3·THF results in the formation of **7** as the single metallaborane product along with BH_2Cl as a coproduct.[18] We suggest $(Cp^*MoBH_3)_2$ as an intermediate as $(Cp^*CoBH_3)_2$ has been identified in the reaction of $(Cp^*CoCl)_2$ with monoboranes leading ultimately to $(Cp^*Co)_2B_3H_7$ and other products.[16] Further, we have shown that $(Cp^*Cr)_2B_4H_8$, **9**, adds borane to yield the chromium analogue of **7** thereby lending credance to a stepwise build-up of the borane fragment in these metallaboranes.[18]

As already indicated in the earlier sections, the reaction of $(Cp^*MoCl_2)_2$ (**2**) with borane gives a more complicated set of products showing that more than a simple reduction of **2** to [CpMoCl] takes place. The discussion is simplified by establishing that reaction of Cp^*MoCl_4 (**1**) with BH_3·THF yields **2** as the sole product. In a reaction of **1** with borane at room temperature, integration of the ^{11}B NMR spectra measured after 90 min shows that the initial step involves the consumption of 2 equiv of BH_3·THF and formation of 2 equiv of BH_2Cl. At

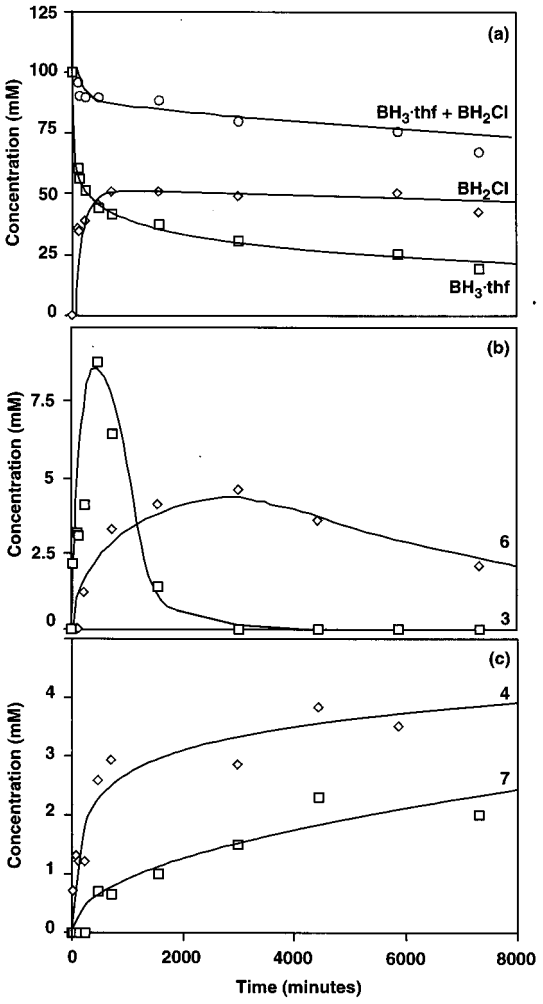

Figure 5. Concentration vs time graphs for reaction mixture 3 (see Table 3) obtained by periodic monitoring of ^{11}B NMR signal intensities: (a) monoboron species; (b) intermediates **3** and **6**; and (c) final products **4** and **7**.

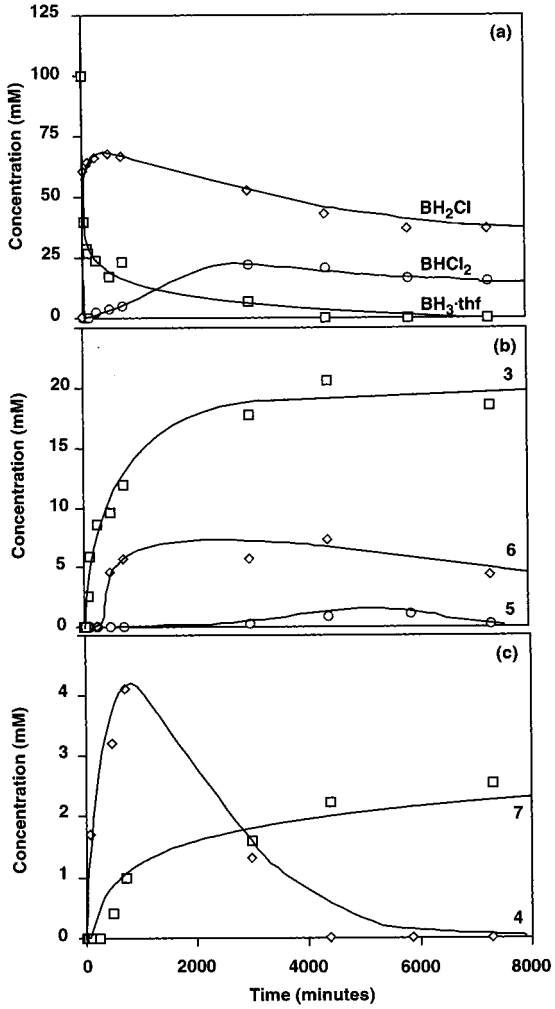

Figure 6. Concentration vs time graphs for reaction mixture 1 (see Table 3) obtained by periodic monitoring of ^{11}B NMR signal intensities: (a) monoboron species; (b) intermediates **3**, **5**, and **6**; and (c) final products **4** and **7**.

the same time all of the purple Cp*$MoCl_4$ suspended in the toluene disappears, gas is evolved, and the resulting solution is brown in color. These results taken together with the finding that **1** and **2** give near identical mixtures of products under similar conditions show that the initial step in the reaction sequence is reduction of **1** to **2** via reaction 1

$$\text{Cp*MoCl}_4\ (\mathbf{1}) + 2\text{BH}_3\cdot\text{THF} \rightarrow {}^1/_2(\text{Cp*MoCl}_2)_2\ (\mathbf{2}) + 2\text{BH}_2\text{Cl} + \text{H}_2 \quad (1)$$

This is corroborated by ^{1}H NMR monitored experiments that reveal the growth of signals due to **2** in the same time span. For convenience, then, **1** was used in the detailed NMR experiments described next.

Three ^{11}B NMR-monitored reactions were carried out in which the ratio of reactants **1**:BH_3·THF was varied between 1:4 and 1:7 (see Table 3). Relevant concentration vs time graphs for the various components of the three different reaction mixtures are reproduced in Figures 5 and 6 (see also Figure 8, Supporting Information). Concentration vs time graphs for the ^{11}B silent components of the ^{1}H-monitored reaction mixture are reproduced in Figure 7. Several features are apparent from analysis of the data. The ^{11}B NMR spectra obtained from reaction mixture 3 are used to generate Figure 5. Figure 5a shows the variation in concentration of the monoboron species

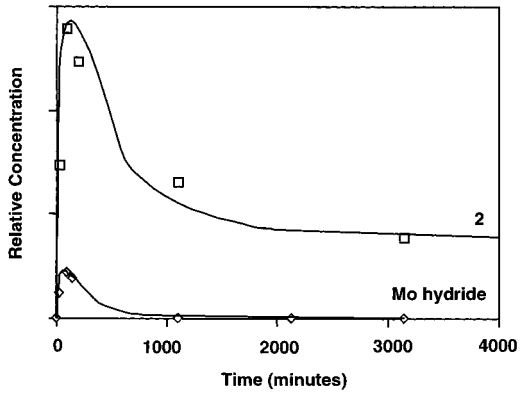

Figure 7. Relative concentration vs time graphs for reaction mixture 1 (see Table 3) obtained by periodic monitoring of ^{1}H NMR signal intensities: ^{11}B NMR silent species $(Cp*MoCl_2)_2$ (**2**) and a molybdenum hydride intermediate.

BH_3·THF and BH_2Cl. As expected BH_3·THF is consumed, and its concentration diminishes sharply with a corresponding growth in the concentration of BH_2Cl. The total concentration of monoboron species decreases with time as the amount of boron incorporated within the various metallaboranes increases. Figure 5, parts b and c shows how the concentrations of the intermediates **3** and **6** and the two final products $(Cp*MoCl)_2B_4H_{10}$ (**4**)

and $(Cp^*Mo)_2B_5H_9$ (**7**) vary with time. The concentrations of **4** and **7** show the expected concentration/time behavior, and it is noteworthy that **4** appears to be the first formed of the two. For $t < 1000$ min the concentration of **4** is greater than that of **7** by at least a factor of 3, and only at longer reaction times does the ratio appear to diminish noticeably. Of the intermediate species, **3** is the first to be detected; its concentration reaches nearly 10 mM after 480 min but dies away to zero after 4000 min. **6** is formed much later in the course of the reaction, reaching its maximum of concentration at ca. 2500 min and is not fully consumed even after 8000 min. No other borane containing species are observed during the course of the reaction.

Analogous concentration/time graphs for reaction mixture 1 (containing less BH_3·THF) are shown in Figure 6 and reveal different time-dependent behavior. First, the concentrations of the species **3** and **6** do not die away completely due to the insufficient amounts of BH_3·THF present, which prevents complete reaction to **4** and **7**. In addition, the intermediate $(Cp^*MoCl)_2B_3H_7$ (**5**) is clearly detected in this reaction mixture, albeit at low concentration peaking at around $t = 600$ min. **5** was barely detectable in reaction mixtures containing higher concentrations of BH_3·THF. If the cluster expansion proceeds from **5** to **7** by addition of two BH fragments and loss of Cl (as BH_2Cl), then the rate of loss of **5** will depend strongly on the concentration of BH_3·THF. Only when the rate of the cluster expansion step is slowed significantly by reducing the amount of BH_3·THF available is the highly reactive unsaturated species **5** detected.

The other major difference between reaction mixtures 1 and 3 is that the concentrations of two species which appeared to be ultimate products in reaction 3 [BH_2Cl and $(Cp^*MoCl)_2B_4H_{10}$ (**4**)] reach maxima and then begin to diminish. In reaction mixture 1 the concentration of **4** decays to zero at $t = 4400$ min and is accompanied by a similar decrease in the concentration of BH_2Cl; however no resonances attributable to new metallaboranes were observed to grow in. Possibly **4** reacts with BH_2Cl to yield a molybdenum chloride species (rather than a metallaborane); cluster degradation yielding metal halide products has previously been observed to occur in the reaction of $(Cp^*Cr)_2B_4H_8$ with species containing a B−Cl bond.[45] This assertion was confirmed by an independent experiment; reaction of **4** with BH_2Cl in toluene under reaction conditions similar to those used above resulted in consumption of **4** over a 2 week period and the detection of no new metallaborane products by ^{11}B NMR.

The results of the ^1H NMR-monitored experiment yield similar concentration/time behavior for the metallaboranes **3**−**7** to those obtained by ^{11}B NMR spectroscopy under the same conditions. Figure 7 depicts concentration vs time behavior for ^{11}B silent species—$(Cp^*MoCl_2)_2$ (**2**) and a second unknown species which gives rise to a resonance at δ_H −11.5 with no apparent coupling to ^{11}B in the ^1H NMR and which has no corresponding ^{11}B signal. This species is observed during the early stages of the reaction and subsequently dies away, showing behavior characteristic of a reaction intermediate. It is possible that this signal is due to some form of molybdenum hydride—although the resonance is broader than might be expected for an Mo-*H* species.[46] The signal is certainly in the correct region of the spectrum for a hydrogen-bridged Mo−*H*−Mo linkage [*cf.* −12.23 for the bridging hydrogen in Cp_2-Mo(μ-Cp)(μ-H)Mo(H)Cp[47] and −11.45 for $CpMo(CO)_2(\mu$-H)(μ-I)$Mo(CO)_2Cp$[48]], and the signals for both molybdenum-bound protons in $Cp_2Mo(\mu$-Cp)(μ-H)Mo(H)Cp are described by Green et al. as "broad."[47] It is certainly not out of the question that a bridging hydride could feature in the early stages of the reaction pathway from Cp^*MoCl_4 to $(Cp^*Mo)_2B_5H_9$ although it is difficult to state this with confidence on the basis of these observations.

Scheme 3

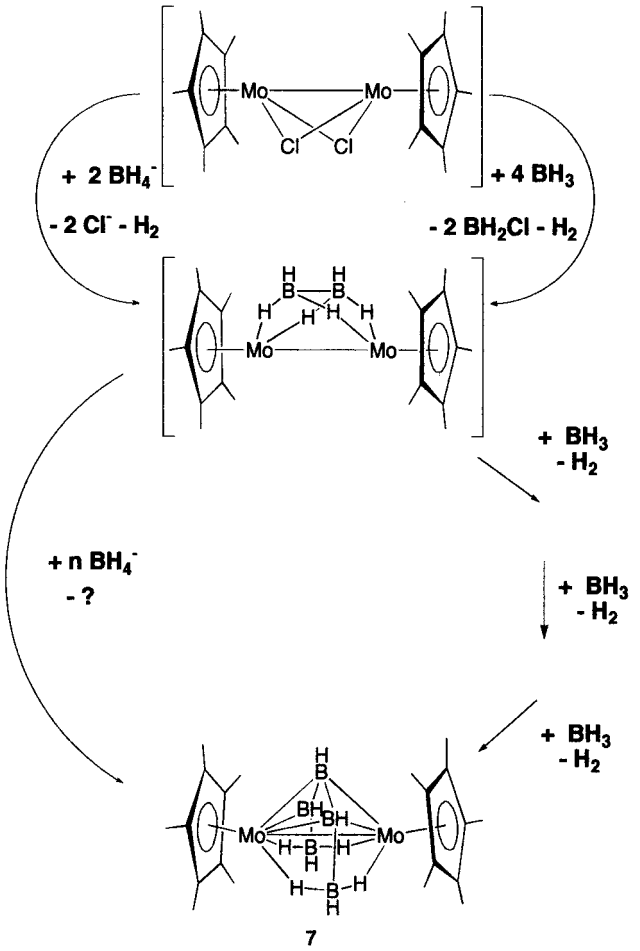

The summaries of the borane reactions in Schemes 1 and 3 require no further comment; however, that in Scheme 2 does. In the reaction of BH_3·THF with **1** three competing reactions which consume the key intermediate **3** are proposed to account for the observations. First, reaction to give **4** is irreversible, and since **4** is unreactive toward further BH_3·THF (but reactive to BH_4^-—see below), a product is isolated in which not all of the chloride ligands have been replaced by borane units. Formation of **4** from **3** by replacement of a terminal BH unit by $B(B_2H_5)$ is an unusual reaction, but one which finds precedent in the formation of $[B_5H_8][B_2H_5]$ and $[1,6\text{-}C_2B_4H_5][B_2H_5]$ from B_5H_9 and $1,6\text{-}C_2B_4H_6$, respectively.[49] Second, insertion of a BH unit into the B_2H_6 fragment of **3** can generate the reactive intermediate **5** (and ultimately the Mo_2B_5 species **7**). Third, replacement of the remaining two bridging chlorides in **3** by B_2H_6 to give **6** also takes place, and appreciable concentrations of **6** are observed in the reaction mixtures; reaction of **6** with

(45) Aldridge, S.; Shang, M.; Fehlner, T. P. *Acta Crystallogr*. In press.
(46) See, for example: Jesson, J. P. In *Transition Metal Hydrides*; Muetterties, E. L., Ed.; Marcel Dekker Inc.: New York, 1971; p 87.
(47) Bashkin, J.; Green, M. L. H.; Poveda, M. L.; Prout, C. K. *J. Chem. Soc., Dalton Trans* **1982**, 2485.
(48) Curtis, M. D.; Fotinos, N. A.; Han, K. R.; Butler, W. M. *J. Am. Chem. Soc*. **1983**, *105*, 2686.
(49) Corcoran, E. W.; Sneddon, L. G. *J. Am. Chem. Soc.*, **1985**, *107*, 7446.

BH_3·THF is slow, such that appreciable amounts of **6** persist in solution even after 6 days at 55 °C [see Figure 5b].

The proposal of **3** as an intermediate common to formation of both **5** and **6** is consistent with the concentration/time behavior for all three species seen in Figure 5. Furthermore, the idea that **5** is formed from **3** is consistent with the observation [Figure 6b] that the concentration of **5** builds up to appreciable levels only when the concentration of **3** is high (so that the rate of formation of **5** is high) and the concentration of BH_3·THF is low (so that the rate of consumption of **5** is low). Insertion of BH into a B_nH_{n+4} fragment to give a $B_{n+1}H_{n+5}$ unit finds precedent in the cluster expansion reaction of $(Cp^*Cr)_2B_4H_8$ to $(Cp^*Cr)_2B_5H_9$ with $BHCl_2$·SMe_2 or BH_3·THF.[11,18] For the same reason, $(Cp^*Mo)_2B_4H_8$ is postulated as an intermediate species leading from **5** to **7**.

Borohydride. A summary of the results for this monoborane is also included in Schemes 1−3. The reaction of $LiBH_4$ with [Cp*MoCl] prepared in situ from **2** and $[Et_3BH]^-$ yields only **7**. This was unexpected, and it is not clear how the presumed $(Cp^*MoBH_3)_2$ intermediate is converted into **7** by borohydride. Other products must be involved and the best route to a product mixture containing **7** alone remains the reaction of borane with [Cp*MoCl]. Note that in the case of the reaction of $(Cp^*CrCl)_2$ with borohydride, $(Cp^*CrBH_4)_2$ is the sole product at room temperature, and only on heating is **9** produced in a mixture of products some of which are paramagnetic.[8]

As with borane, reduction of **1** by BH_4^- leads exclusively to **2** and is accompanied by the release of BH_3·THF, according to reaction 2

$$Cp^*MoCl_4\ (\mathbf{1}) + 2LiBH_4 \xrightarrow{\text{toluene/THF}} {}^1/_2(Cp^*MoCl_2)_2\ (\mathbf{2}) + 2BH_3\cdot THF + 2LiCl + H_2 \quad (2)$$

The NMR experiments show that in the presence of a large excess of $LiBH_4$, **2** then reacts with 2 equiv of BH_4^- to generate **3** (with release of H_2) which then reacts with 2 further equiv to generate **6**. This chemistry is completely analogous to that observed for the corresponding niobium and tantalum systems, in which Cp′M(μ-Cl)$_4$MCp′ is converted to Cp′M(μ-B_2H_6)$_2$-MCp′ via the intermediate Cp′M(μ-Cl)$_2$(μ-B_2H_6)MCp′ [M = Nb, Cp′ = C_5Me_4Et; M = Ta, Cp′ = C_5Me_5], i.e., by stepwise replacement of pairs of chloride ligands by $B_2H_6^{2-}$.[30,32]

Further reaction of **6** to **7** is very slow, as demonstrated by the minimal conversion at 55 °C over a period of several weeks. On the other hand, if 3.5 equiv of BH_4^- are used, the 2 equiv consumed in the initial reduction of **1** to **2** results in a low concentration of BH_4^- in solution after the next step (i.e., formation of **3** from **2**). Consequently the rate of conversion of **3** to **6** (which would be expected to be dependent on the concentration of BH_4^-) will be lower, and the concentration of **3** remaining will be higher. This is observed to be the case. Moreover, with 2 equiv of BH_3·THF being generated in the initial reduction step, reaction of **3** with BH_3·THF will compete with the reaction with BH_4^-. **3** could thus react with BH_3·-THF and be converted via **5** into **7**. This would then account for the larger amount of **7** produced when 3.5 equiv of $LiBH_4$ are used rather than 10. Note, however, that **7** is synthesized in far greater yield from **1** when BH_3·THF is used.

The completely different products produced by the reaction of **2** vs [Cp*MpCl] with borohydride shows that reduction of **2** to [Cp*MoCl] by BH_4^- is not competitive with the reactions shown in Scheme 2. Thus, although both monoborane reagents take **1** to **2** they are not sufficiently reducing to produce [Cp*MpCl] on the time scale of the cluster building reactions.

Although one of the final products $(Cp^*MoCl)_2B_4H_{10}$ (**4**) is unreactive toward BH_3·THF and can be isolated from the Cp^*MoCl_4/BH_3·THF reaction mixture, it does react with BH_4^-. The bis(B_2H_6) adduct **6** is formed together with a small amount of **7**. As indicated in reactions 3 and 4 replacement of bridging

$$(Cp^*MoCl)_2B_4H_{10} + 2LiBH_4 \xrightarrow{\text{toluene/THF}} (Cp^*MoH)_2B_4H_{10} + 2BH_3\cdot THF + 2LiCl \quad (3)$$

$$(Cp^*MoH)_2B_4H_{10} \rightarrow (Cp^*Mo)_2(B_2H_6)_2 \quad (4)$$

chlorides with hydrides by BH_4^- to give $(Cp^*MoH)_2B_4H_{10}$ is followed by rearrangement to give $(Cp^*Mo)_2(B_2H_6)_2$ (**6**). An attractive alternative route by which the pendant B_2H_5 is clipped off to produce **3** and $[B_3H_8]^-$ followed by reaction of **3** with additional $[BH_4]^-$ to give **6** was ruled out as no $[B_3H_8]^-$ was observed as a product.

Role of the Ancillary Ligand: Cp vs Cp*. To investigate the possible role of the Cp* ligand (electronic and steric) the analogous reactions of the Cp starting materials **1′** and **2′** with BH_3·THF were carried out. These give only a single metallaborane end product identified by the spectroscopic data as $(CpMo)_2B_5H_9$ (**7′**). In addition, only one intermediate species is detected; given the extremely similar spectra measured for this species and the Cp* intermediate **3** it is identified as $(CpMoCl)_2B_2H_6$ (**3′**). The reaction is considerably more facile in the Cp case, complete conversion to the final product **7′** being accomplished in 3 days at room temperature (in contrast to the 55 °C temperature and 6 day reaction times required in the Cp* case). No Cp compounds analogous to the Mo(III) metallaboranes **4** and **5** or to the bis(B_2H_6) species **6** were detected. In the Cp* case three reaction pathways are observed from the intermediate **3**. The differing chemistry of the Cp and Cp* derivatives suggests that in the Cp case addition of extra BH fragments to the intermediate **3′** (to give **5′** and hence **7′**) is much more facile than for Cp*. Consequently this route is the predominant one, and CpMo clusters analogous to **4** and **6** are not observed. If addition of BH fragments to the borane framework is more facile for Cp than Cp*, then one might reasonably expect the Cp analogue of **5** to be even more reactive than its Cp* counterpart, and it never attains a concentration high enough to be observed by ^{11}B NMR.

On electronic grounds one would expect the more electron rich Cp*Mo species to be more reactive toward electrophilic species such as BH_3; it seems likely therefore that the higher reactivity of the Cp species is based on steric rather than electronic grounds. Build-up of the borane cage by addition of successive BH fragments to **3** or **3′** would be expected to be easier in the sterically less crowded CpMo dimers.

BH_3·THF vs BH_4^-. Much of the known chemistry of early transition metal monocyclopentadienyl halides involves reaction with nucleophiles or Lewis bases.[50] The observed reactivity of $[BH_4]^-$ is consistent with these observations. It now appears, however, that high oxidation state early transition metal species (such as Cp^*TaCl_4[51] and Cp^*MoCl_4) also exhibit significant reactivity toward electrophilic reagents such as BH_3·THF. The initial step in the reaction may involve interaction of the BH_3 unit with one of the chloride ligands to give a coordinated BH_3-Cl fragment. In fact, selected chloride salts are found to react

(50) See, for example, Poli, R. *Chem. Rev.* **1991**, *91*, 509.
(51) Aldridge, S.; Hashimoto, H.; Shang, M.; Fehlner, T. P. *J. Chem. Soc., Chem. Commun.* **1998**, 207.

with borane to give chloroborohydride ion.[52] Elimination of BH_2Cl could then occur (as is observed experimentally) leaving a metal hydride intermediate. A hydride intermediate $(Cp^*TaCl_2)_2H_2(BH_3)$ *is* observed in the tantalum system, and a ^1H signal at δ_H −11.5 observed in the molybdenum system displays a concentration/time behavior consistent with that of a hydride intermediate early in the reaction scheme. Elimination of H_2 could then complete the necessary reduction of the metal center, whereas addition of another equivalent of borane could lead to metallaborane products.

For Cp^*MX_n species in lower oxidation states borohydride generates metal borohydrides rather than hydrides, and these eliminate hydrogen to give metallaboranes such as **3** and **6**. On the other hand, the Lewis acidity of the borane fosters cluster condensation which competes with chloride abstraction/reduction so that "mixed" species containing both borane fragments and chloride ligands are obtained (e.g., molybdaboranes **3**−**5**). In the case of both chromium and molybdenum the final product is a metallaborane [$(Cp^*Cr)_2B_4H_8$ or $(Cp^*Mo)_2B_5H_9$] in which all chloride ligands have been replaced; the difference in products produced is attributed to larger kinetic barriers to cluster expansion in the chromium case.

As illustrated in Schemes 1−3, one set of products is accessible via either borane or borohydride. The coordination ability of borane, however, leads to facile cluster expansion and a greater variety of metallaborane products. Although the broad outline of reactivity illustrated in the schemes is clear, the mechanistic details are not, e.g., in the conversion of **5** to **7** the stage at which Cl is lost will only be learned from more detailed mechanistic studies.

Conclusions

Both monoborane reagents act in a dual role in which their characteristic reducing properties and coordination abilities lead to both similarities and differences in the products produced from reaction with a given monocyclopentadienylmetal chloride. Based on this work as well as earlier studies, borane seems to be the more versatile reagent for cleanly generating metallaboranes, but both reagents have distinct value, e.g., the best route to **6** is via $[BH_4]^-$, whereas the best route to **7** is via BH_3·THF.

The intermediate $(Cp^*MoCl)_2B_3H_7$ (**5**) represents the second reported example of an unsaturated metallaborane cluster, and the first for which direct comparison is possible with a saturated later transition metal species containing the same borane fragment. **5** contains no multiple bonding between the molybdenum centers and has too few skeletal atoms to adopt a structure based on a polyhedron with fewer vertexes, these being typical responses to electron deficiency in organometallic and cluster chemistry, respectively. The unsaturation in **5** must be delocalized over the cluster framework.

Comparison with $(Cp^*Co)_2B_3H_7$ shows that the existence of a metal−metal bond together with the elevation of M−B antibonding orbitals resulting from a better metal−borane energy match are vital in stabilizing a structure with two fewer electron pairs than the cobalt counterpart. Similar behavior observed for $(Cp^*Cr)_2B_4H_8$ identify this as a more general phenomenon in which a good energy match between metal and borane fragment orbitals can elevate the energy of a M−B skeletal orbital such that the cluster can support one fewer skeletal bonding pair than predicted.

Acknowledgment. The support of the National Science Foundation is gratefully acknowledged. S.A. also thanks the J. William Fulbright Scholarship Board for the award of a research scholarship.

Supporting Information Available: Tables of crystal data, positional and equivalent isotropic thermal parameters, bond distances and angles, and general displacement parameter expressions and Figure 8, the NMR data for reaction mixture 2, Table 3 (27 pages). See any current masthead page for ordering and Web access instructions.

JA973720N

(52) Lawrence, S. H.; Shore, S. G.; Koetzle, T. F.; Huffman, J. C.; Wei, C.-Y.; Bau, R. *Inorg. Chem.* **1985**, *24*, 3171.